



## Numerical Comparison between MSRC and AC based on a Radiated Susceptibility Test

Raghad Hashim Fadhil AL-Saedi<sup>1,\*</sup>, Ibrahim EL-Baba<sup>2</sup>, Jafaar Mohammed Daif Alkhasraji<sup>1</sup>, Dhuha Radhi Nayyef<sup>3</sup>, Abdulkareem Abdulwahab<sup>3</sup>, Khidhair Jasim Mohammed<sup>3</sup>, Ahmed H. Janabi<sup>3</sup>

<sup>1</sup> Department of Electromechanical Engineering, University of Technology, Baghdad, Iraq

<sup>2</sup> Faculty of Technology, Lebanese University, Saida, Lebanon

<sup>3</sup> Air Conditioning and Refrigeration Techniques Engineering Department, Al-Mustaqlab University College, Babylon 51001, Iraq

---

### ARTICLE INFO

**Article history:**

Received 20 July 2025

Received in revised form 29 November 2025

Accepted 10 December 2025

Available online 25 December 2025

---

### ABSTRACT

This study involves a comparison of the experimental findings obtained from testing conducted in the Mode Stirred Reverberation Chamber (MSRC) and the Anechoic Chamber (AC). Directly comparing the reactions of different items under test proved challenging due to variations in the electromagnetic surroundings for both procedures. The tests conducted in both rooms have exhibited varying responses based on the equipment's directivity. Furthermore, the outcomes derived from this examination exhibit variability contingent upon the conditions under which the test is conducted. Hence, the test results obtained from the two chambers exhibit similar error biases. The error bias refers to the proportion of a measured response obtained under specified test conditions compared to the maximum possible reaction. The paper examines the coupling uncertainty and anticipated error bias for both test procedures, analyzing how they vary with apparent directivity. The measured AC data is utilized to ascertain the magnitude and configuration of the apparent directivity of equipment responses.

**Keywords:**

Mode Stirred Reverberation Chamber (MSRC); Anechoic Chamber (AC); Electromagnetic Compatibility (EMC)

## 1. Introduction

AC and MSRC are extensively used test methodologies for EMC radiated immunity testing. An optimal alternating current source provides illumination to the Equipment Under Test (EUT) with a wide range of horizontal and vertical polarizations. It emits multiple plane waves with specific field amplitudes and an adequate variety of incident angles. Nevertheless, testing that adheres to standards restricts the quantity of incident angles [1]. Presently, we employ this test to assess immunity, quantify the shielding effectiveness of an EUT, and gauge emission levels. The AC can recognize the radiation pattern by enhancing the immune response and effectiveness of the bladder or by detecting emissions from an EUT. This computation requires that the tested equipment be exposed to a large quantity of plane waves in all directions and polarizations while in free space.

---

*Corresponding author*

*E-mail address:* 11591@uotechnology.edu.iq

<https://doi.org/10.37934/sej.11.1.94101>

Optimal examinations A Multiple Source Radiated Compliance (MSRC) test involves doing multiple separate tests, each representing different sites within a brewery. In this scenario, the electromagnetic field that illuminates the EUT is both statistically isotropic (uniform in all directions) and homogeneous (uniform in all locations). The maximum intensity of the field is a random variable, but its anticipated value may be predicted. Today, we are specifically focusing on comparing the results obtained by MSRC with those obtained via AC [2]. Both forms of testing have their own set of advantages and limits [3,8]. A major issue in AC testing is to ensure the utilization of the most crucial directions and polarizations, as conventional tests limit their number. However, the specific shape and size of the wave that triggers the electromagnetic interference are known with certainty [4]. Alternatively, the MSRC activates all deficits in the EUT at the same time, which makes it difficult to discern the orientations and polarizations of the waves that cause excitement. Consequently, applying test results to enhance the efficiency of an EUT's shielding is challenging. Nevertheless, because of their cavity resonant properties, MSRCs lack the ability to generate high-intensity fields using a little amount of injected power [5,9,10].

The subsequent sections aim to contrast the functioning of AC and MSRC. Following the completion of a radiated susceptibility test, the equipment utilizes digital computation to analyze and evaluate the electromagnetic field. The next section outlines the numerical model of the AC, which is more intricate compared to that of the MSRC. Upon careful analysis of the data, we suggest a novel approach for harnessing MSRC. This entails integrating temporal methodologies into EMC testing, wherein we subject the EUT to a focused electromagnetic field of significant magnitude over a specific duration. We analyze the benefits of using AC to understand and control the direction and polarization of the wave that affects the EUT. Additionally, we employ the MSRC-approved high field intensity to calculate the radar's effective diffraction section or total effective section [6,11,12].

### 1.1 Theoretical Field PDFs

The hypothesis posits that within an ideal parallel-piped cavity, the mode simulation yields a sinusoidal pattern for the distribution of the field. Nevertheless, their volume constitutes a minuscule fraction of the cavity. When subjected to electromagnetic impact, the sinusoids experience random fluctuations in their amplitude, following a statistical distribution known as "Chi-Square ( $\chi^2$ )."<sup>1</sup> To comprehend this characteristic, it is necessary to represent the electromagnetic field as a complex variable [6,13-15]. Subsequently, the three Cartesian components of the electric field can be expressed in the following manner:

$$E_{(X)} = E_{xr} + i \cdot E_{xi} \quad (1)$$

$$E_{(Y)} = E_{yr} + i \cdot E_{yi} \quad (2)$$

$$E_{(Z)} = E_{zr} + i \cdot E_{zi} \quad (3)$$

Each of these intricate components is the aggregate of many random variables that represent the amplitudes (assumed to be independent) of all the modes.

$$E_x = \sum_{m,n,p} E_{xr}^{m,n,p} + i \cdot \sum_{m,n,p} E_{xi}^{m,n,p} \quad (4)$$

$$E_y = \sum_{m,n,p} E_{yr}^{m,n,p} + i \cdot \sum_{m,n,p} E_{yi}^{m,n,p} \quad (5)$$

$$E_z = \sum_{m,n,p} E_{zr}^{m,n,p} + i \cdot \sum_{m,n,p} E_{zi}^{m,n,p} \quad (6)$$

The six components have the function F1 Eq. 8 for distribution function and for probability density. The variable x's standard deviation  $\zeta$  is represented by F1 Eq. 9.

$$[E_{xr}] = [E_{xi}] = [E_{yr}] = [E_{yi}] = [E_{zr}] = [E_{zi}] = 0 \quad (7)$$

$$f_i(x) = \frac{1}{s\sqrt{2\pi}} e^{-\frac{x^2}{2s^2}} \quad (8)$$

$$F_1(x) = \frac{1}{2} \left[ 1 + erfc \left( \frac{x}{s\sqrt{2}} \right) \right] \quad (9)$$

$$X(t) = E_b e^{-t} \quad (10)$$

## 2. Numerical Modeling

The methodology employed in this section involved the utilization of the Finite Difference Time Domain (FDTD) technique for conducting the simulation. To ensure simplicity, we did the computation in a two-dimensional domain (TM mode) with a predetermined calculation domain  $CD = 1.8 \times 1.8 \text{ m}^2$ . The excitation signals employed represent Gaussian Eq. 10 with a maximum frequency of  $f_{\max} = 3 \text{ GHz}$ , calculated at  $-20 \text{ dB}$ , and an amplitude of  $E_0 = 377 \text{ V/m}$ . We employed a consistent spatial discretization method  $d_x = d_y = 1 \text{ cm}$  that aligns with  $\frac{\lambda f_{\max}}{10}$ , where  $\lambda$   $f_{\max}$  is the wavelength corresponding to  $f_{\max}$ , the wavelength  $\lambda$  and a time step  $dt$  of approximately 23.59 picoseconds. An EUT figure refers to an item that is represented by PECs (Perfect Electric Conductors) and dielectrics, and it includes apertures [16-18].

The objective is to quantify the electric field strength ( $E_z$ ) at a specific location within the EUT after conducting the radiated susceptibility tests using both Alternating Current (AC) and Modulated Sweep Rate Control (MSRC). The AC was simulated using wall circumstances, which act as absorbing boundary conditions for the test. The EUT is subjected to 800 plane waves with two polarizations, which were uniformly distributed across the EUT, resulting in 400 occurrences.

A total of 800 simulations were conducted to record the electric field at a specific point within the EUT for each instance. The MSRC was simulated using the Hill plane wave model [6, 19, 20], where the internal electromagnetic environment was created by combining a limited number of random plane waves. This study employed the Finite-Difference Time-Domain (FDTD) method to simulate a susceptibility test conducted in a reverberant chamber.

Figure 1 displays the form of the transmitted wave, illustrating the arrival of plane waves at varying time intervals. We have successfully mitigated all the instances of time delay Eq. 10.

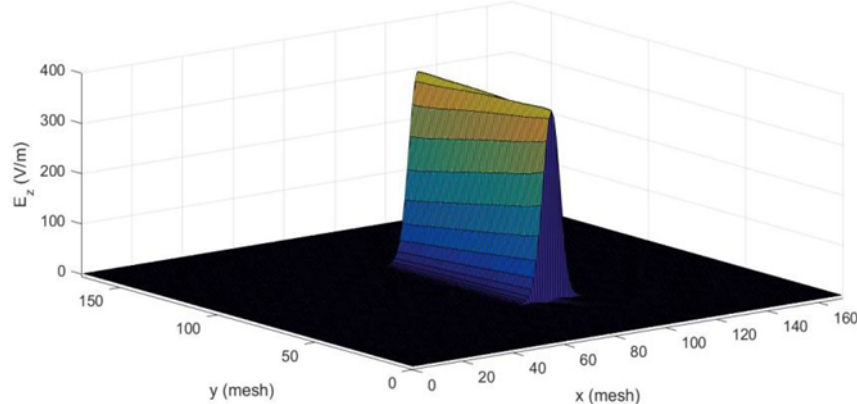


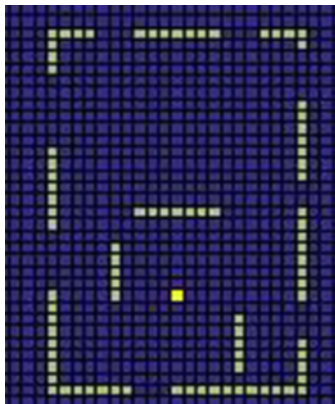
**Fig. 1.** Transmitted plan wave

### 3. Results and Discussion

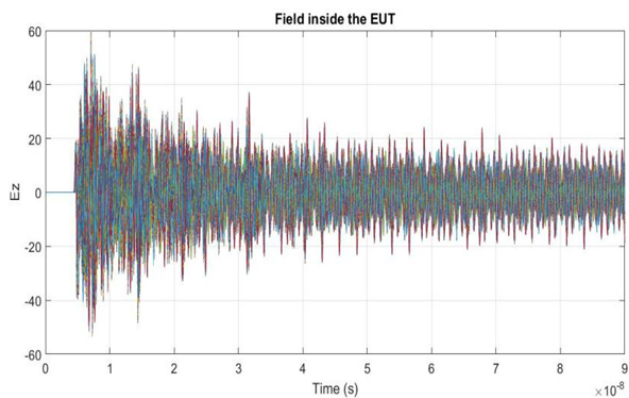
The AC findings are quantified in relation to bias error Eq. 11 [7,12,22], which represents the measured value of the electric field within the EUT.

$$(|E_{RC}|) = \frac{15}{16} \sqrt{\frac{\pi}{3}} \sqrt{N_{OP}} E_0 \quad (11)$$

In Figure 3, we witness a specific occurrence that has been normalized by the maximum value of the field recorded after all events.

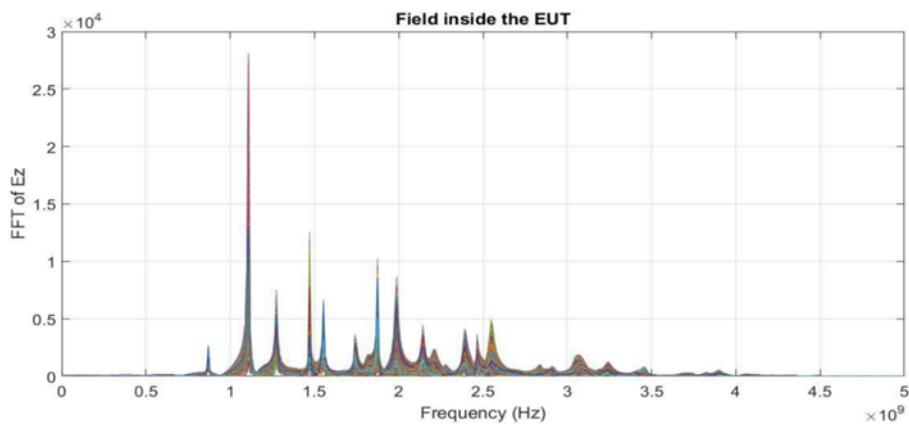


**Fig. 2.** E UT



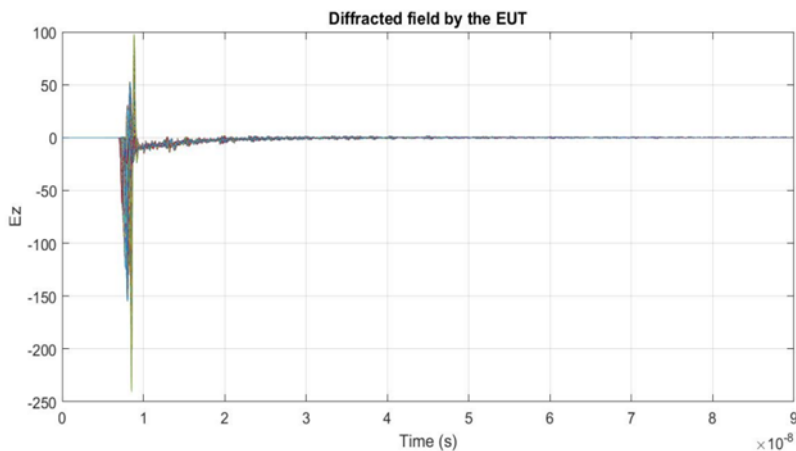
**Fig. 3.** AC chamber and the electric field inside the EUT

Figure 4 displays the spectrum that was measured during the EUT for the electric field.



**Fig. 4.** Spectrum of electric field inside of the equipment under test

Furthermore, it is evident that the diffraction field is observable in the  $E_z$  direction, as depicted in Figure 5.



**Fig. 5.** The diffracted field by the EUT in  $E_z$  direction

Figure 6 shows that the frequency is 1 GHz. The angle of incidence where we have the biggest received field corresponds to a value of 0 dB, while the angle of incidence where the received field is least corresponds to a value of -3 db. The angles of incidence 0°, 90°, 180°, and 270° are perpendicular to the four faces of the EUT.

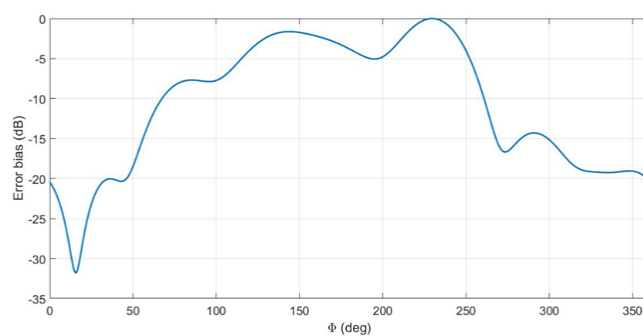


**Fig. 6.** Received electric

This estimate may be subject to multiple sources of uncertainty. By restricting the selection of incidence angles, such as in experimental tests where we sometimes choose angles that line with the EUT's faces, there is a potential danger of disregarding the most prevalent critique of the EUT. For our situation, the crucial orientation for EUT is 212°, which does not correspond to any of the four sides of the object in question.

Consequently, the directivity's true value may exceed previous assumptions. In addition, extensively long testing durations are required to evaluate multiple configurations that correspond to distinct occurrences for a complex EUT.

A Multiple-Source Reverberation Chamber determines the cumulative impulse response of the field while keeping the orientation of the EUT unchanged. Nevertheless, similar to AC, identifying the most pivotal orientation can provide a difficulty. Figure 7 displays the normalized spectrum of the electric field  $E_z$ , obtained from the equation below [7]:

$$(|E_{RC}|) = \frac{15}{16} \sqrt{\frac{\pi}{3}} \sqrt{N_{OP}} E_0 \quad (12)$$

At a specific location inside the European Union Treaty in the Multilateral Security and Reconciliation Commission. The frequency response exhibits multiple resonance peaks, which align with the resonance frequencies of the apertures and the EUT.

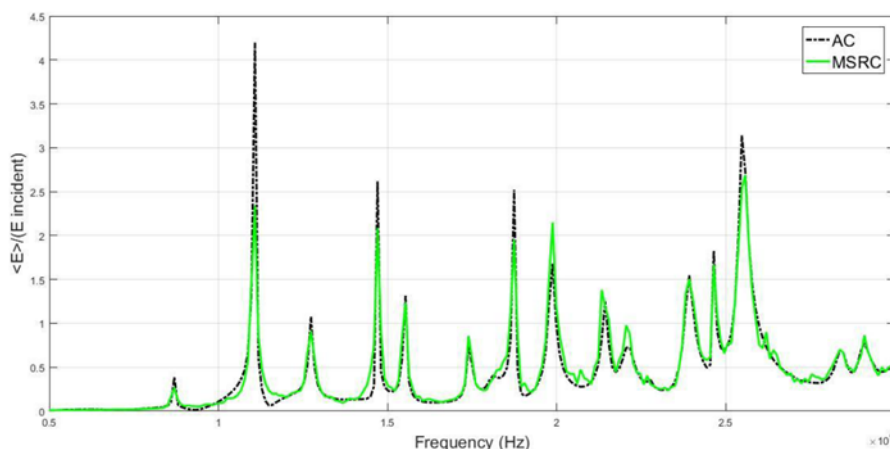


**Fig. 7.** Simulated for the electric field  $E_z$  at a point of the EUT in AC and in MSRC chamber

We confirmed this result by conducting an AC simulation, where we measured the average electric field of all incident plane waves and adjusted it based on the spectrum of the incident plane wave. There is a strong correlation between the MSRCRC and AC models in terms of resonance frequency levels and amplitudes.

#### 4. Conclusions

The purpose of this study was to utilize the advantages of two complementary testing methods, MSRC and AC, to carry out pulsed radiated susceptibility investigations. We performed multiple numerical simulations to showcase the efficiency and accuracy of our method, which is not influenced by losses caused by the RC or its structure. In addition, the preliminary research enabled us to conduct multiple Electromagnetic Compatibility (EMC) applications in the MSRC and make comparisons between its features and those of Alternating Current (AC). The categorization based on industry-standard tests contradicts the temporal domain delineation. After establishing the

brewers' accreditation, a new method is introduced to achieve selective focusing in the system, allowing for the testing of radiated sensitivity.

## References

- [1] Lalléchère, Sébastien, Sébastien Girard, David Roux, Pierre Bonnet, Françoise Paladian, and Alain Vian. "Mode stirred reverberation chamber (MSRC): A large and efficient tool to lead high frequency bioelectromagnetic in vitro experimentation." *Progress In Electromagnetics Research B* 26 (2010): 257-290. <https://doi.org/10.2528/PIERB10062313>
- [2] Hoëppé, Frédéric. "Analyse du comportement électromagnétique des chambres réverbérantes à brassage de modes par l'utilisation de simulations numériques." PhD diss., Lille 1, 2001.
- [3] Alkhasraji, Jafaar Mohammed, Salam W. Shneen, and Mohammed Q. Sulttan. "Reduction of large scale linear dynamic mimo systems using aco-pid controller." *Ingeniería e Investigación* 44, no. 1 (2024): e106657-e106657. <https://doi.org/10.15446/ing.investig.106657>
- [4] Bäckström, Mats, Olof Lundén, and Per-Simon Kildal. "19. Reverberation chambers for emc susceptibility and emission analyses." *Proc. Review of Radio Science* 1999-2002 (2002): 429-452.
- [5] Xu, Qian, and Yi Huang. "Anechoic and Reverberation Chambers: Theory, Design, and Measurements." (2019). <https://doi.org/10.1002/9781119362050>
- [6] Duffy, A., A. Orlandi, and K. Armstrong. "Preliminary study of a reverberation chamber method for multiple-source testing using intermodulation." *IET science, measurement & technology* 4, no. 1 (2010): 21-27. <https://doi.org/10.1049/iet-smt.2009.0008>
- [7] Freyer, Gustav J., and Mats G. Backstrom. "Comparison of anechoic and reverberation chamber coupling data as a function of directivity pattern." In *IEEE International Symposium on Electromagnetic Compatibility. Symposium Record (Cat. No. 00CH37016)*, vol. 2, pp. 615-620. IEEE, 2000. <https://doi.org/10.1109/ISEMC.2000.874691>
- [8] Moglie, Franco, and A. Pia Pastore. "FDTD analysis of plane wave superposition to simulate susceptibility tests in reverberation chambers." *IEEE Transactions on electromagnetic compatibility* 48, no. 1 (2006): 195-202. <https://doi.org/10.1109/TEMC.2006.870793>
- [9] Alkhasraji, Jafaar Mohammed Daif, Ahmed Hameed Reja, Ahmed Mamoon Mahmood, and Manal Hadi Al-Janabe. "Performance improvement of hybrid orthogonal optical signals for small enclosed environments." In *AIP Conference Proceedings*, vol. 3002, no. 1, p. 020001. AIP Publishing LLC, 2024. <https://doi.org/10.1063/5.0205979>
- [10] Kadhim, Riadh A., Qaidar Mohammed Salih, Ashraf Dhannon Hasan, Jafaar Mohammed Daif Alkhasraji, and Hamid Vahed Kalankesh. "D-shaped microfluidic channel bimetallic with a highly sensitive spr ri sensor for a large detection range." *Plasmonics* 19, no. 3 (2024): 1383-1394. <https://doi.org/10.1007/s11468-023-02077-4>
- [11] Sulttan, Mohammed Qasim, Salam Waley Shneen, and Jafaar Mohammed Daif Alkhasraji. "Performance enhancement of large-scale linear dynamic MIMO systems using GWO-PID controller." *Bulletin of Electrical Engineering and Informatics* 12, no. 5 (2023): 2852-2859. <https://doi.org/10.11591/eei.v12i5.4870>
- [12] Alkhasraji, Jafaar, and Charalampos Tsimenidis. "Performance synchronization enhancement of wireless optical communication over pure seawater channel." In *AIP Conference Proceedings*, vol. 2415, no. 1, p. 070001. AIP Publishing LLC, 2022. <https://doi.org/10.1063/5.0092322>
- [13] Al-Ali, Ahmed Kamil Hasan, and Jafaar Mohammed Daif Alkhasraji. "Colour image encryption based on hybrid bit-level scrambling, ciphering, and public key cryptography." *Bulletin of Electrical Engineering and Informatics* 12, no. 3 (2023): 1607-1619. <https://doi.org/10.11591/eei.v12i3.4728>
- [14] Alkhasraji, Jafaar, and Charalampos Tsimenidis. "Performance investigation of coded IM/DD optical OFDM for short range underwater wireless channel." In *AIP Conference Proceedings*, vol. 2415, no. 1, p. 070002. AIP Publishing LLC, 2022. <https://doi.org/10.1063/5.0092326>
- [15] Gros, J-B., Geoffroy Lerosey, Fabrice Mortessagne, Ulrich Kuhl, and Olivier Legrand. "Uncorrelated configurations and field uniformity in reverberation chambers stirred by reconfigurable metasurfaces." *Applied Physics Letters* 118, no. 14 (2021). <https://doi.org/10.1063/5.0041837>
- [16] del Hougne, Philipp, Jérôme Sol, Fabrice Mortessagne, Ulrich Kuhl, Olivier Legrand, Philippe Besnier, and Matthieu Davy. "Diffuse field cross-correlation in a programmable-metasurface-stirred reverberation chamber." *Applied Physics Letters* 118, no. 10 (2021). <https://doi.org/10.1063/5.0039596>
- [17] Monsef, Florian, Andrea Cozza, Dominique Rodrigues, Patrick Cellard, and Jean-Noel Durocher. "Relative variance of the mean-squared pressure in multimode media: Rehabilitating former approaches." *The Journal of the Acoustical Society of America* 136, no. 5 (2014): 2621-2629. <https://doi.org/10.1121/1.4897314>
- [18] Höijer, Magnus, Luk R. Arnaut, and Hans-Georg Krauthäuser. "The Total Electric Field Compared to the Rectangular Component of the Electric Field in a Complex Environment." In *AIP Conference Proceedings*, vol. 1106, no. 1, pp. 66-75. American Institute of Physics, 2009. <https://doi.org/10.1063/1.3117114>

- [19] Serna, Patrick J., and Gary H. Liechty. "Electromagnetic shielding effectiveness of composite material." In *AIP Conference Proceedings*, vol. 458, no. 1, pp. 741-746. American Institute of Physics, 1999. <https://doi.org/10.1063/1.57646>
- [20] Sadeghimalekabadi, Mahyar, Alireza Davari, and Mohaddeseh Fadaei. "Noise reduction in small wind turbines with optimized serrated blades." *Physics of Fluids* 36, no. 5 (2024). <https://doi.org/10.1063/5.0202934>
- [21] Richardson, Benjamin N., Jana Kainerstorfer, Barbara Shinn-Cunningham, and Christopher A. Brown. "Neural mechanisms of spatial auditory attention with magnified interaural level difference cues." *The Journal of the Acoustical Society of America* 155, no. 3\_Supplement (2024): A306-A307. <https://doi.org/10.1121/10.0027601>
- [22] Al-Ali, Ahmed Kamil Hasan, and Fadhil Sahib Hasan. "Efficient energy design of NRPC-CSS under selective Rayleigh fading channel." In *AIP Conference Proceedings*, vol. 3002, no. 1, p. 020013. AIP Publishing LLC, 2024. <https://doi.org/10.1063/5.0205974>